Abrupt Stress Induced Transformation in Amorphous Carbon Films with a Highly Conductive Transition Phase

D. W. M. Lau, D. G. McCulloch, M. B. Taylor, and J. G. Partridge
Applied Physics, School of Applied Sciences, RMIT University, GPO Box 2476V Melbourne 3001, Australia

D. R. McKenzie and N. A. Marks
School of Physics, University of Sydney, New South Wales 2006, Australia

E. H. T. Teo and B. K. Tay
School of Electrical and Electronic Engineering, Nanyang Technological University, Singapore 639798
(Received 21 December 2007; published 28 April 2008)

We demonstrate that when, and only when, the biaxial stress is increased above a critical value of 6 ± 1 GPa during the growth of a carbon film at room temperature, tetrahedral amorphous carbon is formed. This confirms that the stress present during the formation of an amorphous carbon film determines its sp^3 bonding fraction. In the vicinity of the critical stress, a highly oriented graphitelike material is formed which exhibits low electrical resistance and provides Ohmic contacts to silicon. Atomistic simulations reveal that the structural transitions are thermodynamically driven and not the result of dynamical effects.

DOI: 10.1103/PhysRevLett.100.176101 PACS numbers: 68.55.−a, 78.40.Pg, 81.05.Tp

The sharp boundary between *crystalline* forms of carbon, well explored at high pressures and temperatures [1], is exploited in the commercial production of diamond. At room temperature, the transformation of graphite to hexagonal diamond can be induced by pressure alone and is accompanied by a sharp increase in resistivity [2]. In contrast, the *liquid* phase of carbon appears to show a smooth progression in the proportion of the sp^2 to sp^3 hybridized states with increasing pressure, without any phase transition [3]. In *amorphous* carbon (*a*-C), usually prepared as a thin film, it was thought that the boundary between the sp^2-rich and sp^3-rich phases was diffuse because of the amorphous nature of both materials [4]. Furthermore, there is a debate concerning the mechanism of the transition between the sp^2-rich and sp^3-rich phases. Some have argued that stress is not causative [5,6] while others have proposed [7,8] that biaxial stress is analogous to pressure and can drive the transition. Here we provide definitive experimental evidence that an abrupt transition exists between the two amorphous phases and that changes in biaxial stress can drive the transition between them.

Thin films of *a*-C were deposited onto 1–100 Ω-cm *p*-type ⟨100⟩ silicon at room temperature using C ions generated from a dual-bend [9] filtered cathodic arc deposition system [10] operating with a 99.999% pure graphite target at an arc current of 56 A. The silicon substrates were cleaned ultrasonically in pure ethanol, placed in the deposition chamber and pumped down to a base pressure of 6×10^{-6} Torr. The average ion energy for each set of experimental conditions was determined from the plasma potential (measured using a Langmuir probe) and the substrate bias, assuming singly ionized carbon atoms. Mass spectrographic analysis of the ions from a vacuum arc operating under similar conditions has revealed that more than 95% of the ions are singly ionized with the remainder doubly ionized [11]. Carbon films with thicknesses in the range 20–80 nm and different levels of intrinsic stress (calculated by Stoney's equation [12] and using a surface profiler to measure substrate curvature and film thickness) were fabricated by varying the substrate bias as well as the background Ar gas pressure. The films were prepared with breaks of 60 s for every 60 s of deposition. No film delamination was observed. The stress versus ion energy curve (see Ref. [13]) has a maximum in compressive stress in the vicinity of 100 eV, and its shape is typical for energetic growth of thin films. The addition of argon background gas reduces the deposition rate and the stress for a given energy. Auger depth profiling using xenon as the sputtering gas revealed no evidence of incorporated Ar.

Transmission electron microscopy (TEM) and electron energy loss spectroscopy were used to investigate microstructure, density, and bonding configurations. Plan view TEM specimens were prepared by floating the film from the Si substrate in acid. Cross-sectional specimens were prepared by mechanical polishing followed by ion bean thinning. By measuring the plasmon energy loss, the density of the material was calculated assuming a free-electron model and assuming 4 valence electrons per carbon atom [14,15]. The fraction of sp^2 bonded carbon atoms was calculated from the carbon *K*-shell ionization edge [16]. The films showed a linear relationship between sp^2 fraction and density (see Ref. [17]), as previously reported experimentally [4] and theoretically [18] for *a*-C films.

Figure 1(a) plots the film density as a function of stress and shows an abrupt transition region at 6 ± 1 GPa (shown in gray) between a low density phase (containing

 © 2008 The American Physical Society

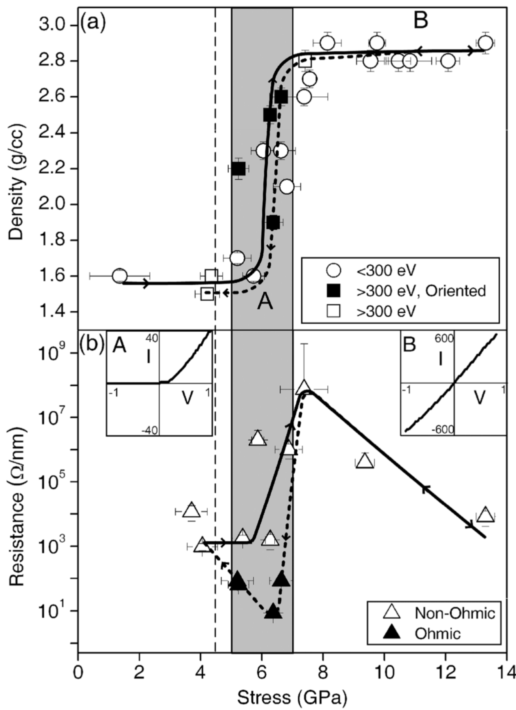

FIG. 1. (a) Density as a function of stress for a-C films prepared with ion energies ranging from 35 to 1000 eV. (b) The through-film resistance per unit thickness as a function of stress. Insets A and B show examples of non-Ohmic and Ohmic current-voltage characteristics, respectively. (a,b) The thin vertical dashed line indicates the predicted transition stress, with the experimental transition region shown in gray. The solid and dashed thick lines show the trajectories through the transition region when the ion energy is increased (see text).

$75 \pm 10\%$ sp^2) and a high density phase (containing $75 \pm 10\%$ sp^3). This high density phase is known as tetrahedral amorphous carbon (*ta*-C) [7] with important applications as a protective medium for magnetic media and optical components. The presence of an Ar background gas during deposition and/or a Cu interface layer did not alter the value of the critical transition stress. Furthermore, the critical stress does not depend on the direction from which the transition region is approached. As energy is increased from thermal values, the transition region is crossed as the stress increases [shown by the solid line in Fig. 1(a)] and the *ta*-C region is entered. Once the maximum stress is reached (approximately 100 eV), further increase in energy causes a lowering of stress and the transition region is reentered [shown as a dashed line in Fig. 1(a)].

This transition between a-C phases is analogous to that between graphite and diamond, which at room temperature occurs at a hydrostatic pressure of approximately 3 GPa [1]. In a-C films, the transition is induced by a biaxial stress that is predicted to be higher than the hydrostatic pressure in the ratio 3:2 [7], that is, at 4.5 GPa as indicated by the vertical dashed line in Fig. 1(a). This value is consistent with the observed onset of the transition region given the uncertainties. An underlying assumption in this work is that the stress applied *in situ* during the film deposition is the same as that measured *ex situ* after growth has stopped. For room temperature carbon growth on silicon, this has been confirmed [19] using an optical lever method in which *in situ* measurements of curvature were compared with *ex situ* measurements.

Figure 1(b) shows the through-film electrical resistance evaluated at a potential of 1 V as a function of stress. At low stress, the resistance is intermediate in magnitude, with an asymmetric, current-voltage characteristic (inset A) resembling that of a Schottky barrier as is often observed for carbon films on silicon [20]. As the stress is increased along the solid line in Fig. 1(b), *ta*-C is formed and the resistance increases by 5 orders of magnitude while maintaining nonlinear behavior. At even higher stresses, a gradual reduction in resistance occurs even though the sp^2 fraction does not change. We suggest a mechanism for this, based on increased hopping driven by stress induced overlap of the localized wave functions associated with the minority sp^2 phase. Hopping conductivity is a dominant mode of conduction in amorphous semiconducting materials [21]. Strikingly different behavior is observed on the return path along the dashed line in Fig. 1(b). The high resistance nonlinear current-voltage behavior is replaced by a low resistance linear current-voltage characteristic indicative of a good Ohmic contact (inset B).

The key to understanding this electrical behavior lies in the microstructure. Figure 2(a) shows a cross-sectional dark-field TEM image of a film in the transition region located on the return path (dashed line) in Fig. 1. The diffraction pattern (inset A) reveals localized graphitic {002} reflections aligned with the plane of the film (one of which is indicated by an arrow). Dark-field imaging using this reflection shows that the microstructure consists entirely of graphitelike sheets aligned normal to the film surface, as seen in the bright field high resolution enlargement in inset B. This orientation is preferred on the basis of energy minimization of turbostratic graphite in a biaxial stress field [22]. A schematic of this microstructure is shown in Fig. 2(b). Films with this preferred orientation are indicated by filled squares in Fig. 1(a) and only occur on the dashed trajectory in Fig. 1. It is these films that exhibit low resistance and Ohmic behavior.

Molecular dynamics simulations of thin-film growth using the environment dependent interaction potential for carbon [23] reveal the origin of preferred orientation. Films were grown using monoenergetic carbon beams, in which five hundred atoms are introduced singly onto a preexisting *ta*-C substrate. The motion associated with each impact and the subsequent thermal spike [24] was followed for approximately one picosecond. Prior to the subsequent impact, the entire system was heated for a further picosecond at temperatures between 1000 and 2500 K. This

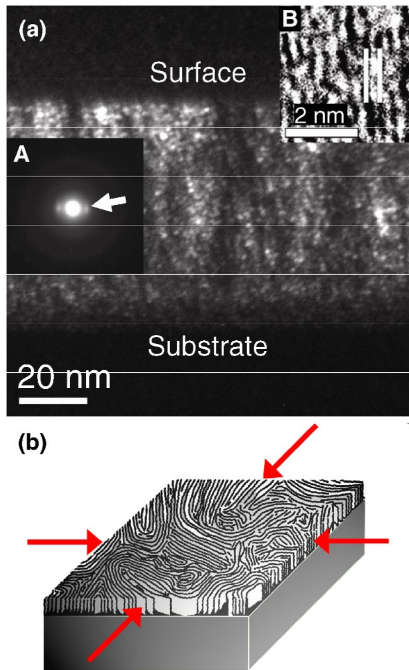

FIG. 2 (color online). (a) Cross-sectional dark-field TEM image of an oriented *a*-C film. This image was taken with an objective aperture centered on the graphitic {002} reflection (arrow in inset A). Inset B shows a high resolution image of the 0.335 nm graphitelike planes (indicated by the vertical white lines) aligned perpendicular to the surface of the film. (b) Schematic representation of the arrangement of sp^2 sheets energetically preferred in a biaxial stress field indicated by arrows.

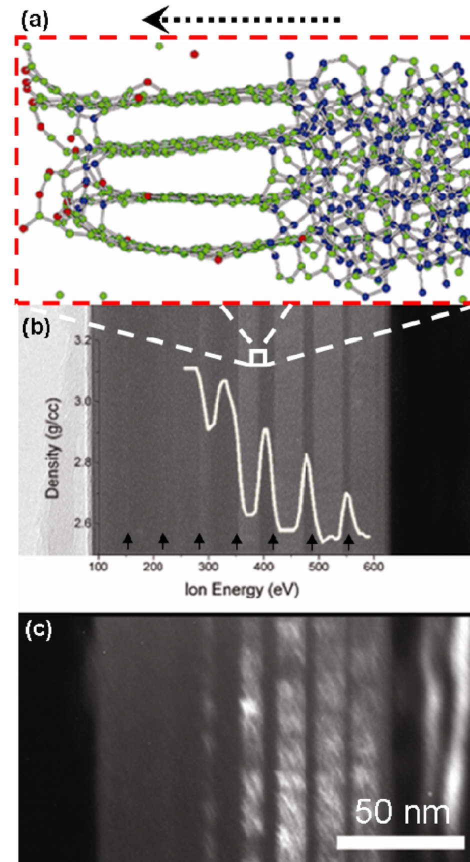

FIG. 3 (color online). (a) Snapshot of a molecular dynamics simulation showing an abrupt change in growth mode between *ta*-C and oriented sp^2 sheets (movie in Ref. [24]). Light gray (light green) atoms are sp^2 while dark gray (dark blue) atoms are sp^3. The growth direction is indicated by the dotted arrow. (b) Cross-sectional TEM image and overlaid density profile of a stress graded *a*-C film deposited by continuously varying the energy from 620 to 95 eV during deposition. The vertical arrows indicate the location of interruptions in film deposition. (c) Dark-field image of (b) taken as in Fig. 2.

temperature-pulsing procedure [25] activates infrequent atomic processes that cannot be modeled on the time scale of standard molecular dynamics. This methodology captures the essential physics of ion deposition, namely, quenched self-annealing on the picosecond time scale *during* thermal spikes and millisecond time scale thermally activated relaxation occurring *between* impacts. Because of computational constraints associated with high energy impacts we cannot perform room temperature depositions at the energy of 300 eV as in the experiments. However, it has been shown experimentally [26] that higher substrate temperatures reduce the ion energy required to drive the transition to ordered carbon. In the simulations, we take advantage of this fact and compensate for our inability to access higher energies by using higher effective substrate temperatures and lower energies (40 and 70 eV).

Figure 3(a) presents a snapshot from a simulation in which infrequent processes are included. The film initially grows as *ta*-C but then abruptly changes growth mode to form sp^2 sheets oriented normal to the film plane (movie in Ref. [27]). When the incident energy is reduced (leading to more rapid quenching), no transition is observed and *ta*-C growth continues indefinitely (movie in Ref. [28]). The sp^2 phase is similarly suppressed when infrequent processes are inhibited by reducing the effective substrate temperature (movie in Ref. [29]). This immediately discounts sputtering and channelling as explanations for the presence of oriented sp^2 structures [6]. Sputtering and channelling are picosecond-scale phenomena which are always observed in the simulations, but the oriented structures only appear when infrequent processes are included.

The simulations demonstrate the combined importance of relaxation on the picosecond and millisecond time scales and show that oriented sp^2 structures arise only when sufficient thermodynamic progress is made towards lower energy configurations. Both relaxation processes act to determine the stress present in the film during growth, and the structural phase that appears is that which has the minimum energy under these stress conditions. Our experiments are fundamentally different from the classic experiments in which graphite is converted to diamond by subjecting it to high pressure at elevated temperature.

Since we are synthesizing solid material from individual atoms in a vapor, the energetically favored phase can appear without the need to cross a large activation barrier. The phase change appears at the boundary between the two phases without the over-pressure normally required.

To confirm the importance of stress in determining the microstructure, a film with an intentionally graded stress was created by linearly varying the ion energy between 620 and 95 eV during growth. This corresponds to the trajectory in Fig. 1(a) from point A to B along the dashed curve, starting in the transition region as an oriented film and crossing the boundary to *ta*-C. Bright and dark-field cross-sectional TEM images shown in Figs. 3(b) and 3(c) confirm that oriented sp^2 sheets only occur in the transition region for energies above 300 eV. Superimposed on Fig. 3(b) is a density profile showing repeated abrupt structural changes between *ta*-C and oriented sp^2 sheets obtained using spectrum imaging with an electron probe approximately 5 nm in diameter. These abrupt changes occur at deliberate interruptions in the growth [indicated by arrows in Fig. 3(b)], necessary to avoid overheating of the carbon source. After growth is recommenced following an interruption, *ta*-C is formed initially and then the oriented sp^2 phase is formed in the subsequent growth. A higher stress in the initial growth of carbon films has previously been observed [18]. The *ta*-C regions become wider and the oriented regions eventually disappear as the stress trends upwards and thermodynamics increasingly favors *ta*-C.

The ability to grow oriented sp^2 sheets at will by controlling the deposition conditions leads to an important application. The graphite sheet is the strongest two dimensional structure known and has high in-plane thermal and electrical conductivity. For this reason, arrays of aligned carbon nanotubes with their axes normal to the plane of the array have been proposed as heat sinks and electrical interconnects. Fully oriented sp^2 sheets as described in this work have all of the advantages of nanotube arrays without the limitations of high deposition temperatures and the need for catalysts.

In summary, we show that a sharp phase boundary exists between the sp^2-rich (graphitelike) and sp^3-rich (diamondlike) forms of *a*-C, analogous to the boundary between graphite and diamond. We demonstrate that when, and only when, the biaxial stress in a film is increased above a critical value of 6 ± 1 GPa during growth at room temperature, the sp^3-rich phase known as *ta*-C is formed. This confirms the role of stress in the formation of this important material that has applications as a protective and optical coating. In the vicinity of the transition stress, a highly oriented graphitelike material is formed, at energies of more than 300 eV, that exhibits low electrical resistance. Although this structure has been observed previously, conditions that create it at room temperature have not been identified until now. Atomistic simulations reveal that this microstructure is thermodynamically driven and is not the result of dynamical effects such as sputtering or channelling.

The authors acknowledge the financial assistance provided by the Australian Research Council (ARC).

[1] F. P. Bundy *et al.*, Carbon **34**, 141 (1996).
[2] R. B. Aust and H. G. Drickamer, Science **140**, 817 (1963).
[3] S. L. Johnson *et al.*, Phys. Rev. Lett. **94**, 057407 (2005).
[4] P. J. Fallon *et al.*, Phys. Rev. B **48**, 4777 (1993).
[5] A. C. Ferrari *et al.*, Diam. Relat. Mater. **11**, 994 (2002).
[6] Y. Lifshitz, S. R. Kasi, and J. W. Rabalais, Phys. Rev. Lett. **62**, 1290 (1989).
[7] D. R. McKenzie, D. Muller, and B. A. Pailthorpe, Phys. Rev. Lett. **67**, 773 (1991).
[8] J. Schwan *et al.*, J. Appl. Phys. **82**, 6024 (1997).
[9] X. Shi *et al.*, Thin Solid Films **345**, 1 (1999).
[10] I. I. Aksenov *et al.*, Sov. J. Plasma Phys. **4**, 425 (1978).
[11] A. Anders, Vacuum **67**, 673 (2002).
[12] G. G. Stoney, Proc. R. Soc. A **82**, 172 (1909).
[13] See EPAPS Document No. E-PRLTAO-100-055817 for a graph of the stress versus ion curve. For more information on EPAPS, see http://www.aip.org/pubservs/epaps.html.
[14] R. F. Egerton, *Electron Energy-Loss Spectroscopy in the Electron Microscope* (Plenum Press, New York, 1996), 2nd ed.
[15] J. T. Titantah and D. Lamoen, Phys. Rev. B **70**, 033101 (2004).
[16] S. D. Berger, D. R. McKenzie, and P. J. Martin, Philos. Mag. Lett. **57**, 285 (1988).
[17] See EPAPS Document No. E-PRLTAO-100-055817 for a graph of the relationship between the sp^2 fraction and density. For more information on EPAPS, see http://www.aip.org/pubservs/epaps.html.
[18] N. A. Marks *et al.*, Phys. Rev. B **65**, 075411 (2002).
[19] M. K. Puchert *et al.*, J. Vac. Sci. Technol. A **12**, 727 (1994).
[20] S. R. P. Silva *et al.*, in *Handbook of Thin Film Materials*, edited by H. S. Nalwa (Academic Press, New York, 2002), Vol. 4, p. 403.
[21] N. F. Mott, *Conduction in Non-Crystalline Materials* (Oxford University Press, New York, 1987).
[22] D. R. McKenzie and M. M. M. Bilek, Thin Solid Films **382**, 280 (2001).
[23] N. A. Marks, Phys. Rev. B **63**, 035401 (2000).
[24] N. A. Marks, Phys. Rev. B **56**, 2441 (1997).
[25] N. A. Marks, M. F. Cover, and C. Kocer, Appl. Phys. Lett. **89**, 131 924 (2006).
[26] M. Chhowalla *et al.*, J. Appl. Phys. **81**, 139 (1997).
[27] See EPAPS Document No. E-PRLTAO-100-055817 for a movie. For more information on EPAPS, see http://www.aip.org/pubservs/epaps.html.
[28] See EPAPS Document No. E-PRLTAO-100-055817 for a movie. For more information on EPAPS, see http://www.aip.org/pubservs/epaps.html.
[29] See EPAPS Document No. E-PRLTAO-100-055817 for a movie. For more information on EPAPS, see http://www.aip.org/pubservs/epaps.html.